Electronic Supplementary Material (ESI) for Dalton Transactions.

Electronic Supplementary Information for:

Mechanism of Intramolecular Transformations of Nickel Phosphanido Hydride Complexes

Shamil K. Latypov,* Fedor M. Polyancev, Yulia S. Ganushevich, Vasily A. Miluykov, Oleg G. Sinyashin

A.E. Arbuzov Institute of Organic and Physical Chemistry of the Russian Academy of Sciences, Arbuzov Street 8, 420088, Kazan, Russia

lsk@iopc.ru

Table of Contents

Experimental Section

All NMR experiments were performed with a 600, 500 and 400 MHz (600.1, 500.1 and 400.1 MHz for ^{1}H NMR; 150.9, 125.8 and 100.6 MHz for ^{13}C NMR; 242.9, 202.5 and 162.0 MHz for ^{31}P NMR, respectively) spectrometers equipped with a 5 mm diameter probehead and a pulsed gradient unit capable of producing magnetic field pulse gradients in the z-direction of 53.5 G·cm^{-1}. Chemical shifts (δ in ppm) are referenced to the solvent toluene-d_8 (δ = 2.09 for ^{1}H and 21.3 ppm for ^{13}C NMR), to external H_3PO_4 (0.0 ppm) for ^{31}P NMR spectra.

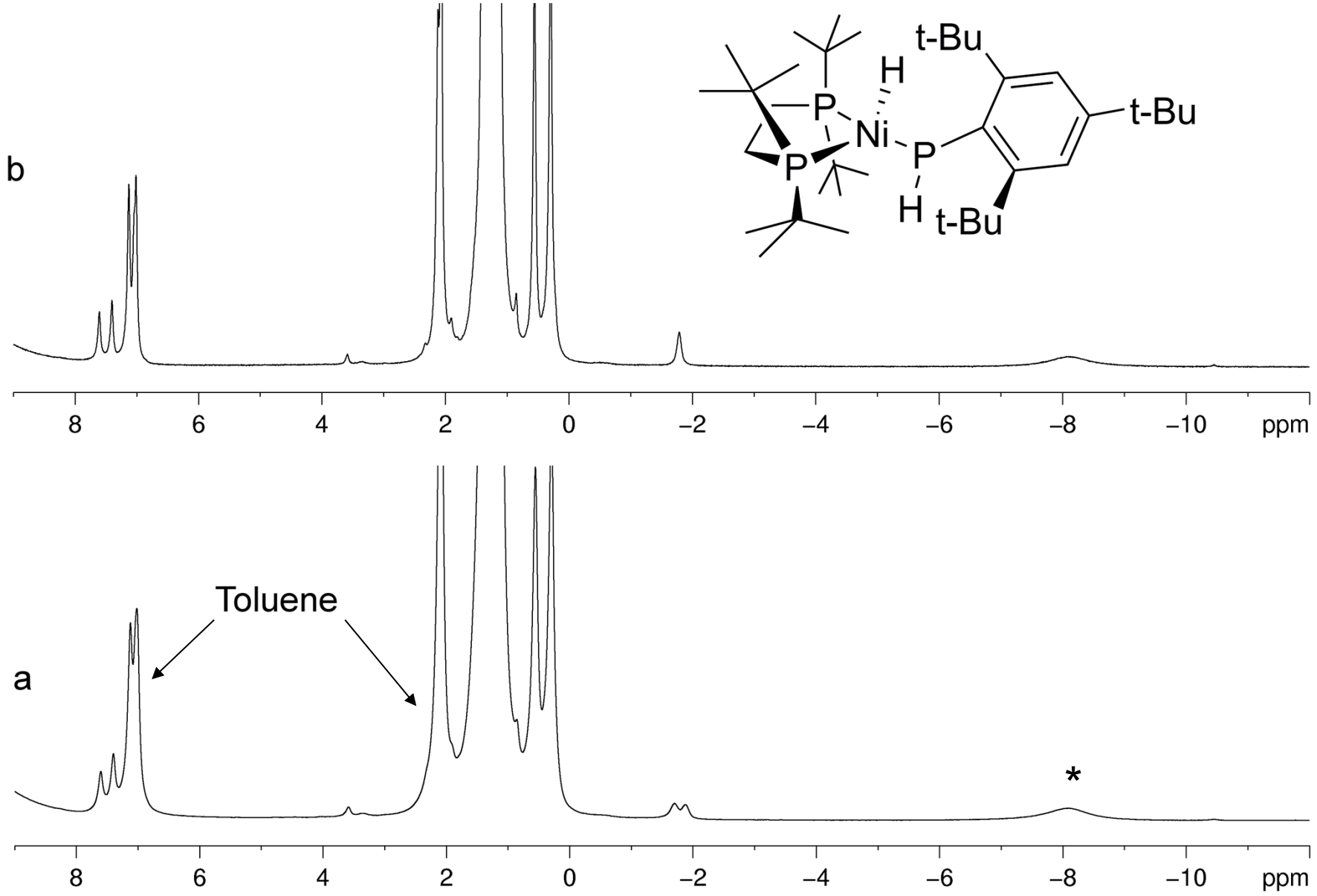

Figure S1. 1D ^{1}H (a) and $^{1}H\{^{31}P\}$ (b) NMR spectra of **2** in toluene-d_8 at T = 303 K (* - unidentified impurty).

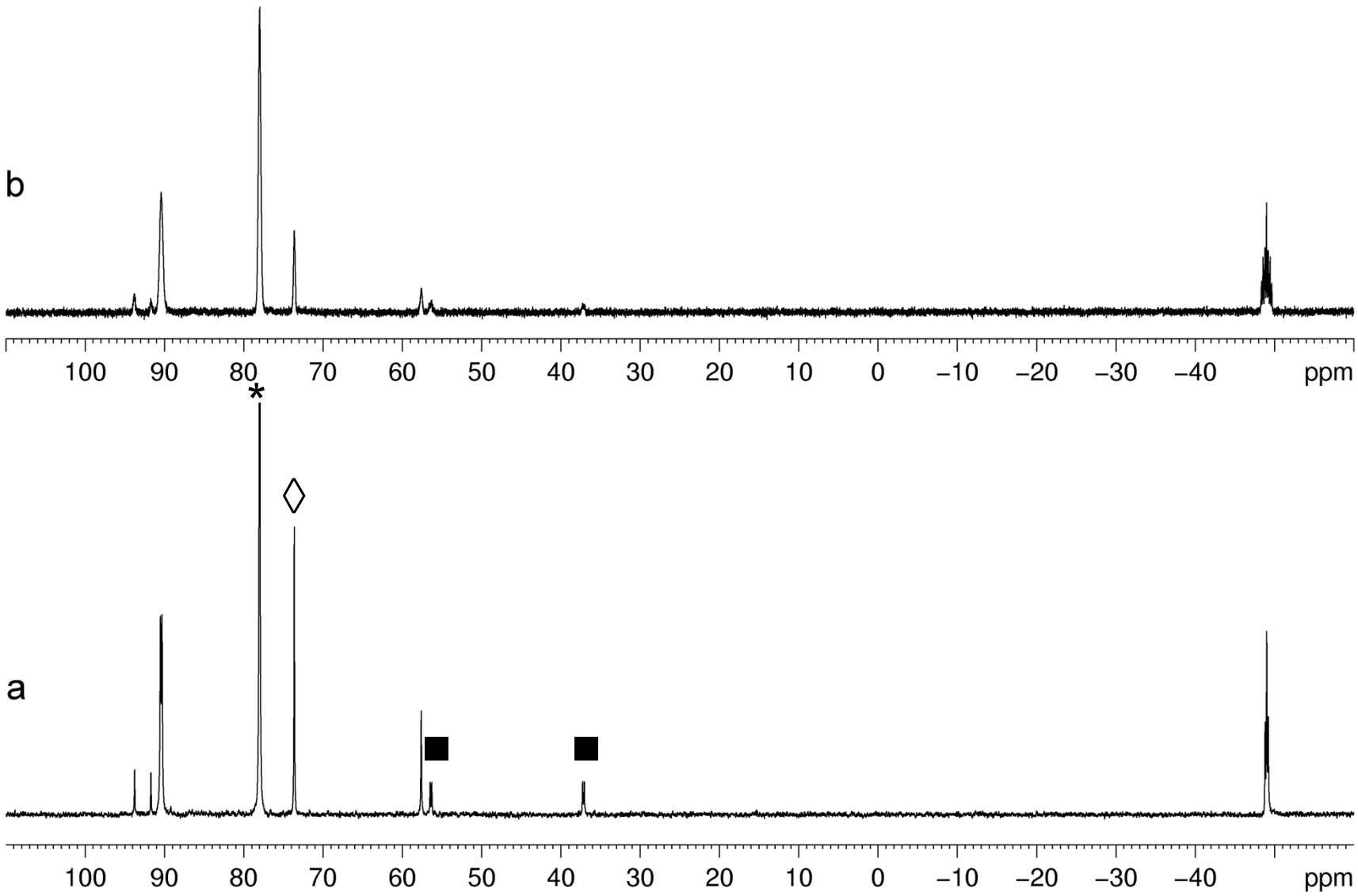

Figure S2. 1D $^{31}P\{^{1}H\}$ (a) and ^{31}P (b) NMR spectra of **2** in toluene-d_8 at T = 303 K (* - [Ni(dtbpe)$(CH_3)_2$, ◊ - [{Ni(dtbpe)}$_2$(μ-η^2:η^2 -$C_6D_5CD_3$)], ■ - $tBu_2P(O)CH_2CH_2PtBu_2$).

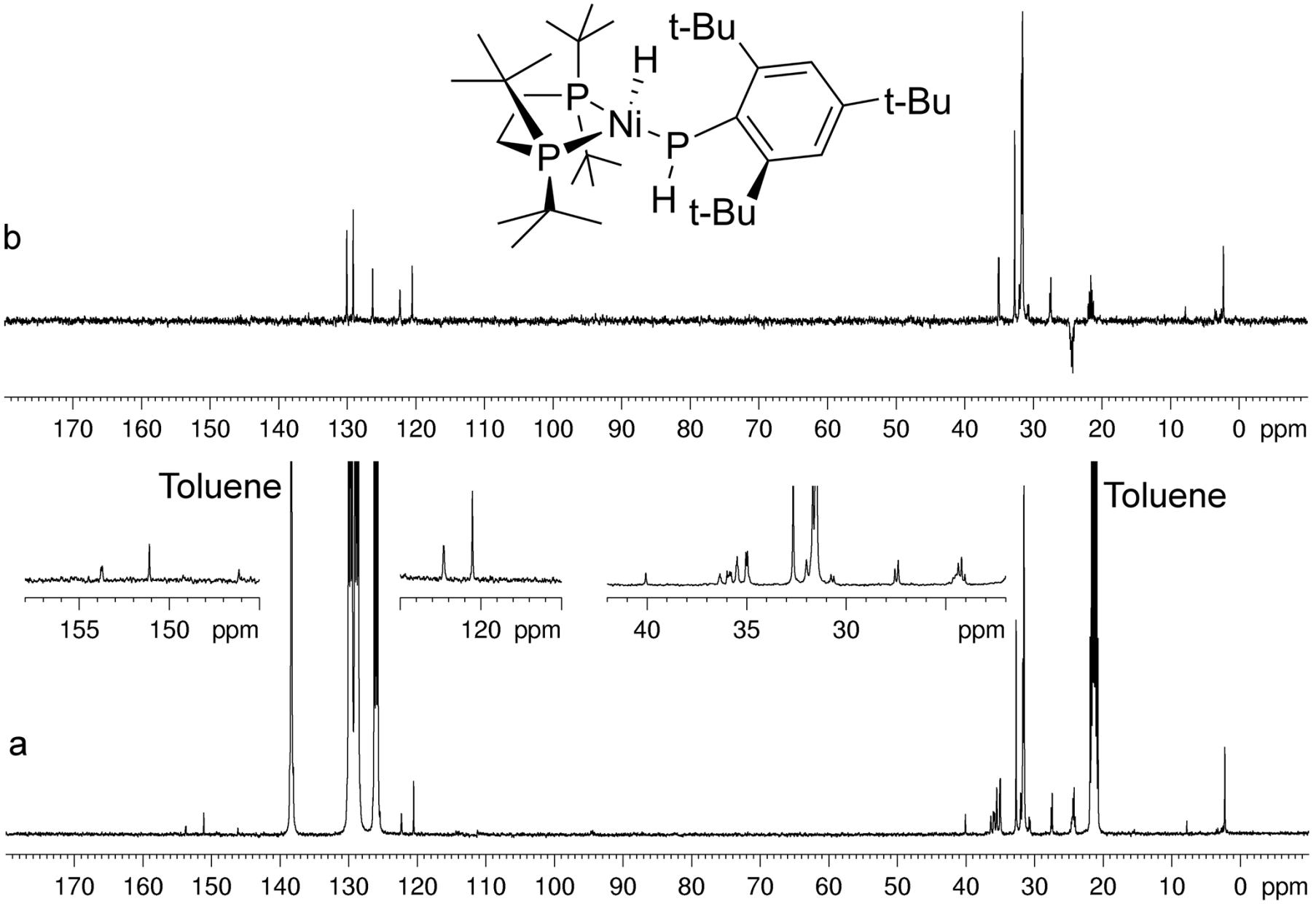

Figure S3. 1D $^{13}C\{^{1}H\}$ and ^{13}C DEPT NMR spectra of **2** in toluene-d_8 at T = 303 K.

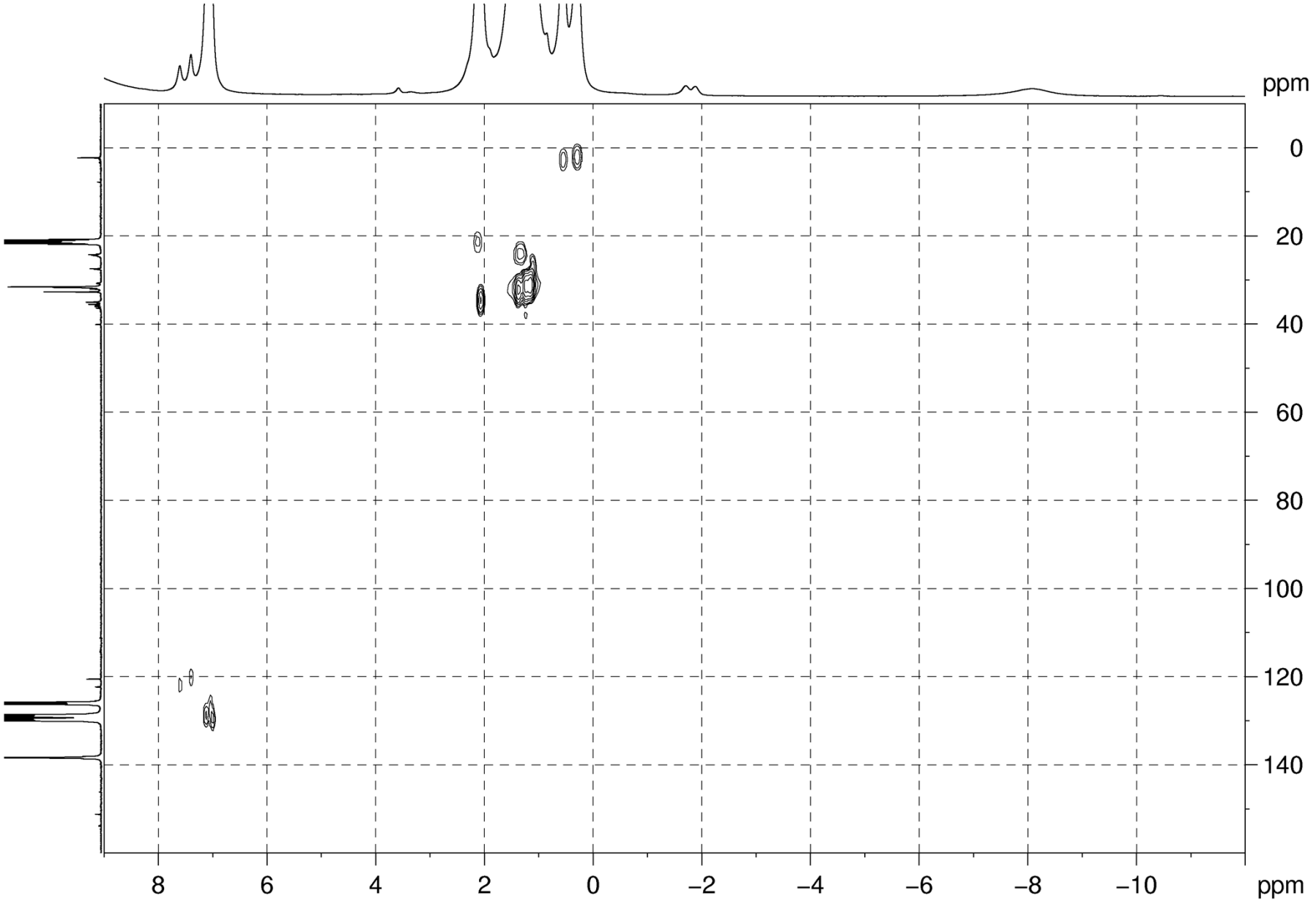

Figure S4. 2D ^{1}H-^{13}C HSQC NMR spectra of **2** in toluene-d_8 at T = 303 K.

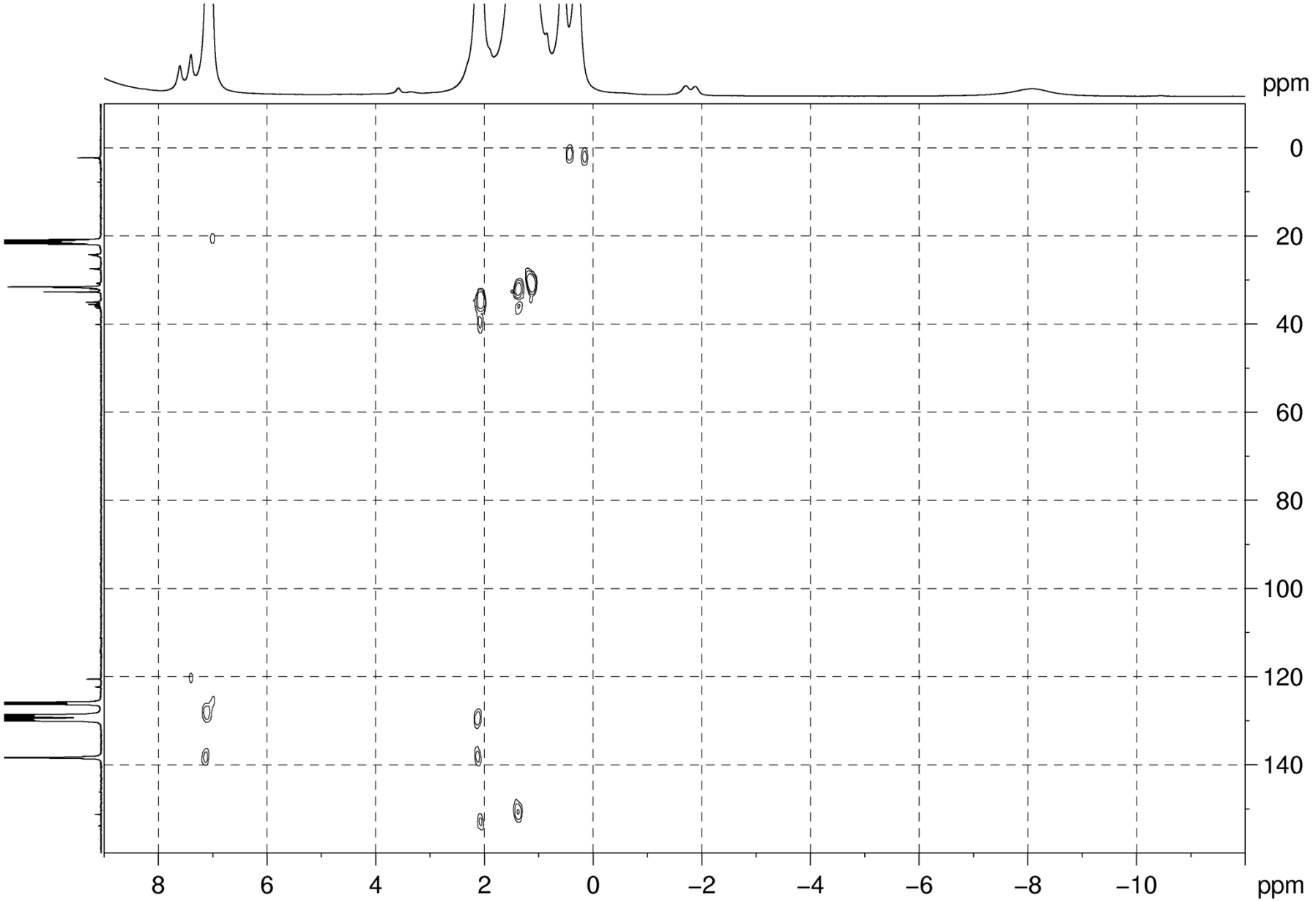

Figure S5. 2D ^{1}H-^{13}C HMBC NMR spectra of **2** in toluene-d_8 at T = 303 K.

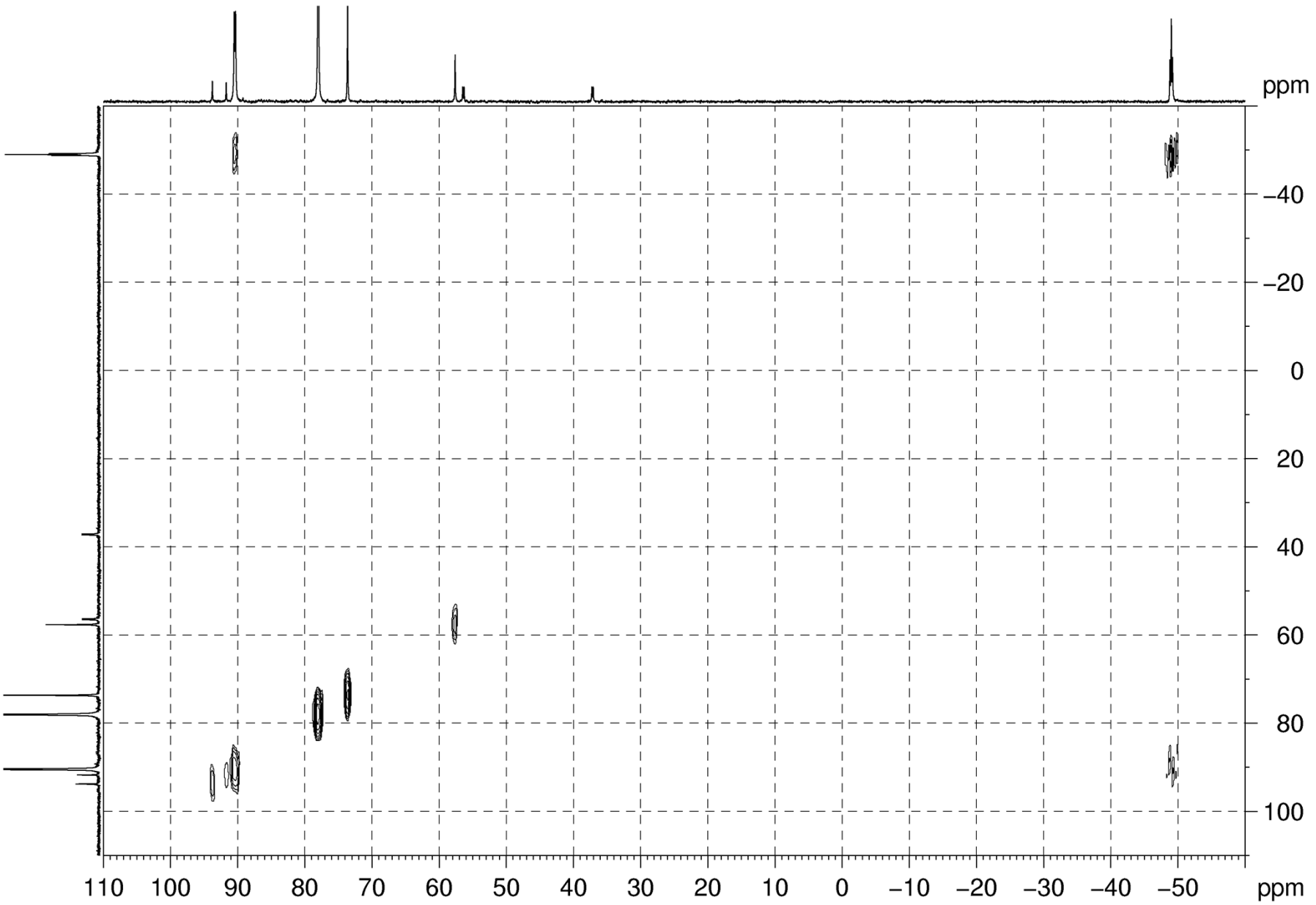

Figure S6. 2D ^{31}P-^{31}P COSY NMR spectra of **2** in toluene-d_8 at T = 303 K.

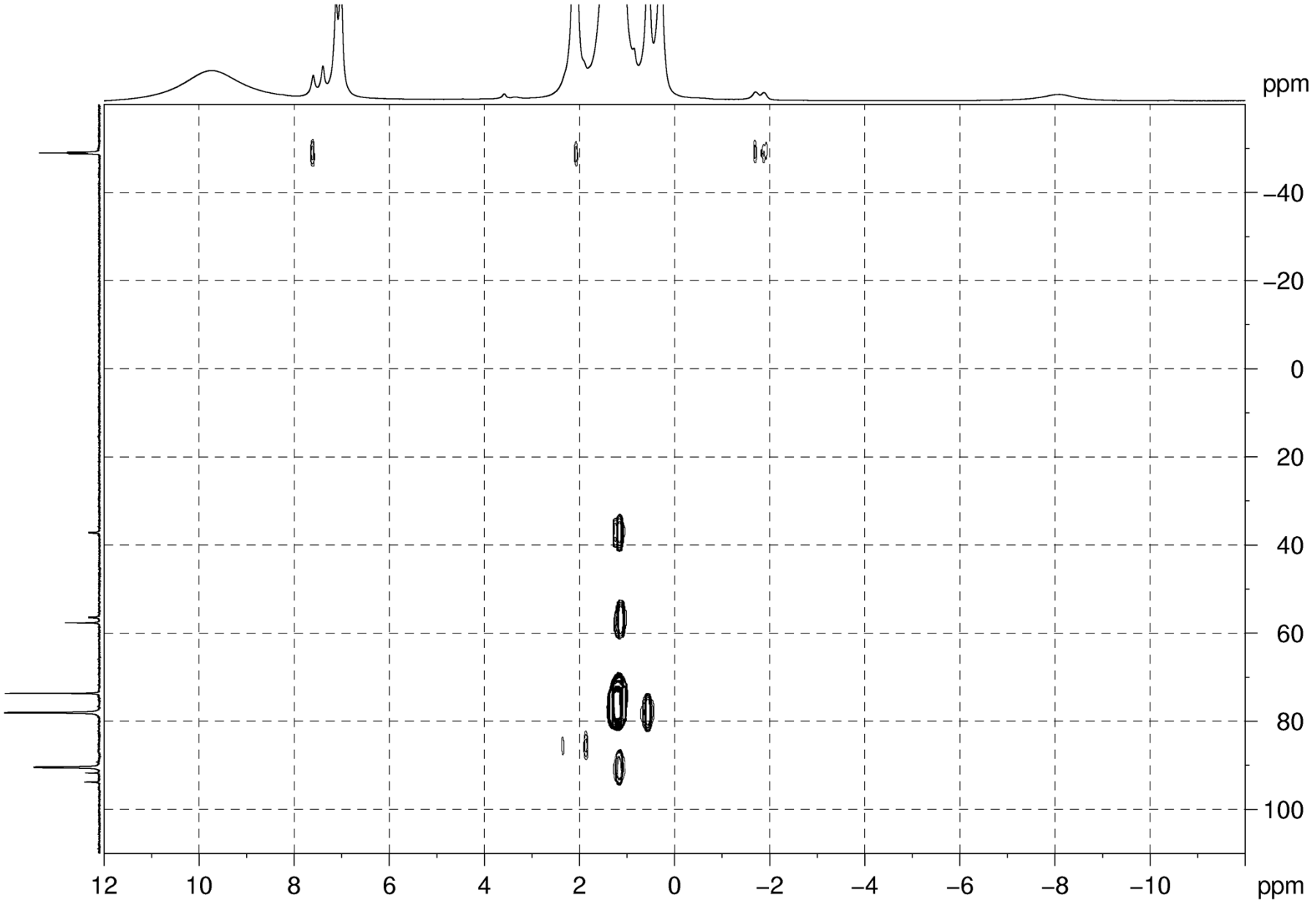

Figure S7. 2D ^{1}H-^{31}P HMBC NMR spectra of **2** in toluene-d_8 at T = 303 K.

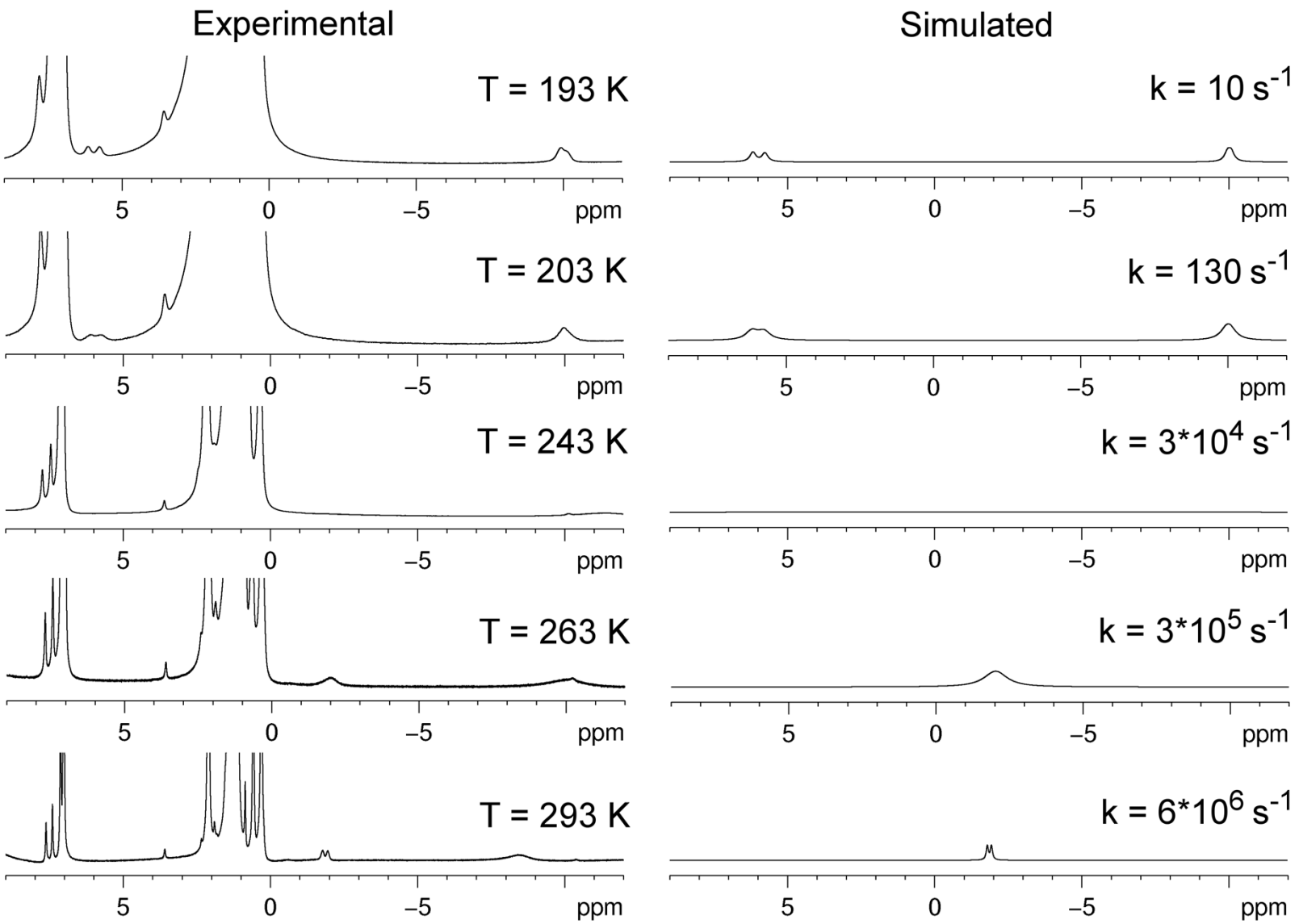

Figure S8. 1D ^{1}H NMR spectra of **2** in toluene-d_8 at different temperatures with corresponding simulated spectra.

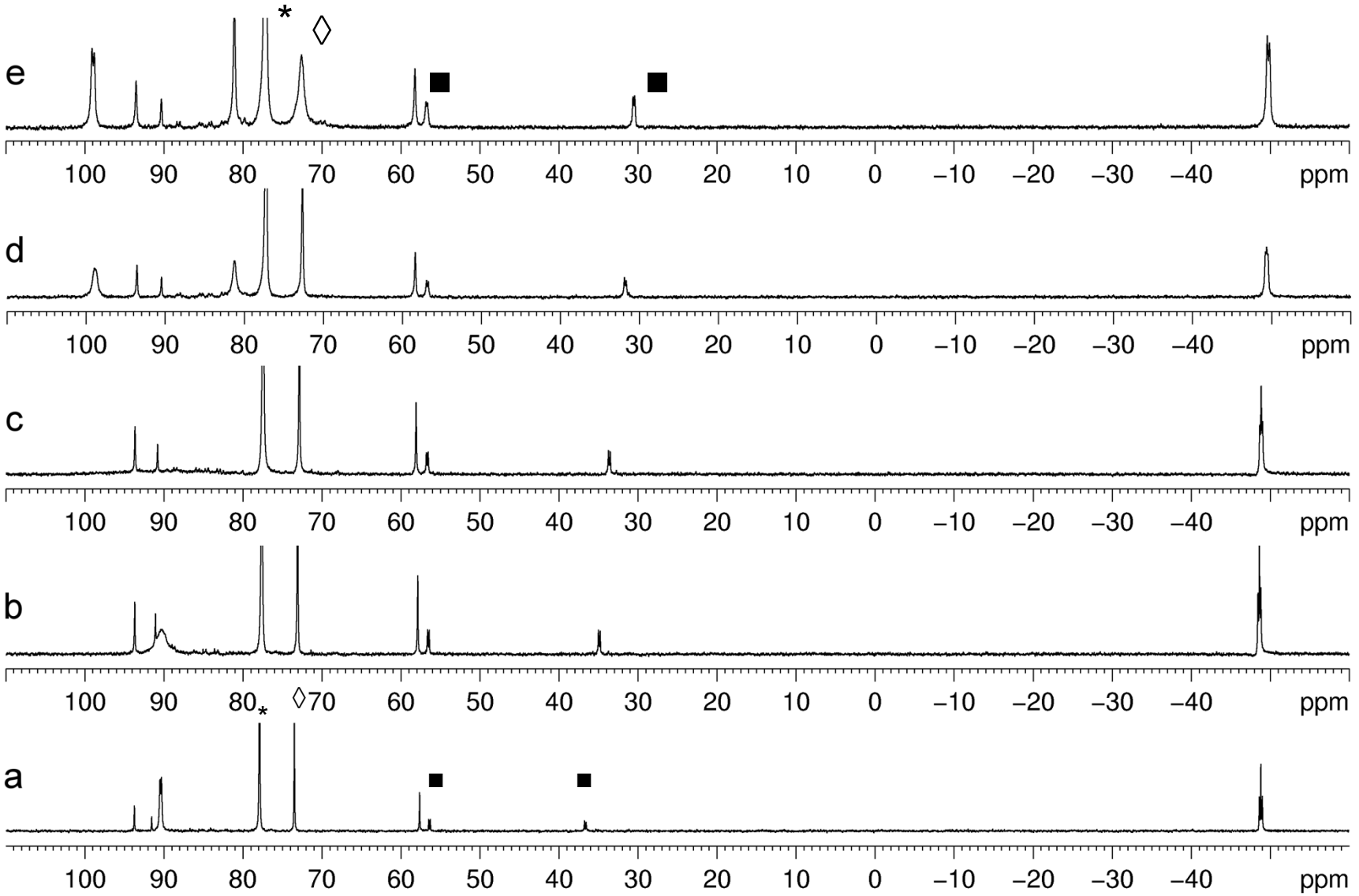

Figure S9. 1D $^{31}P\{^{1}H\}$ NMR spectra of **2** in toluene-d_8 at different temperatures: **a** (T = 293 K), **b** (T = 263 K), **c** (T = 243 K), **d** (T = 213 K), **e** (T = 193 K) (* - $[Ni(dtbpe)(CH_3)_2$, ◊ - $[\{Ni(dtbpe)\}_2(\mu\text{-}\eta^2\text{:}\eta^2\text{-}C_6D_5CD_3)]$, ■ - $tBu_2P(O)CH_2CH_2PtBu_2$).

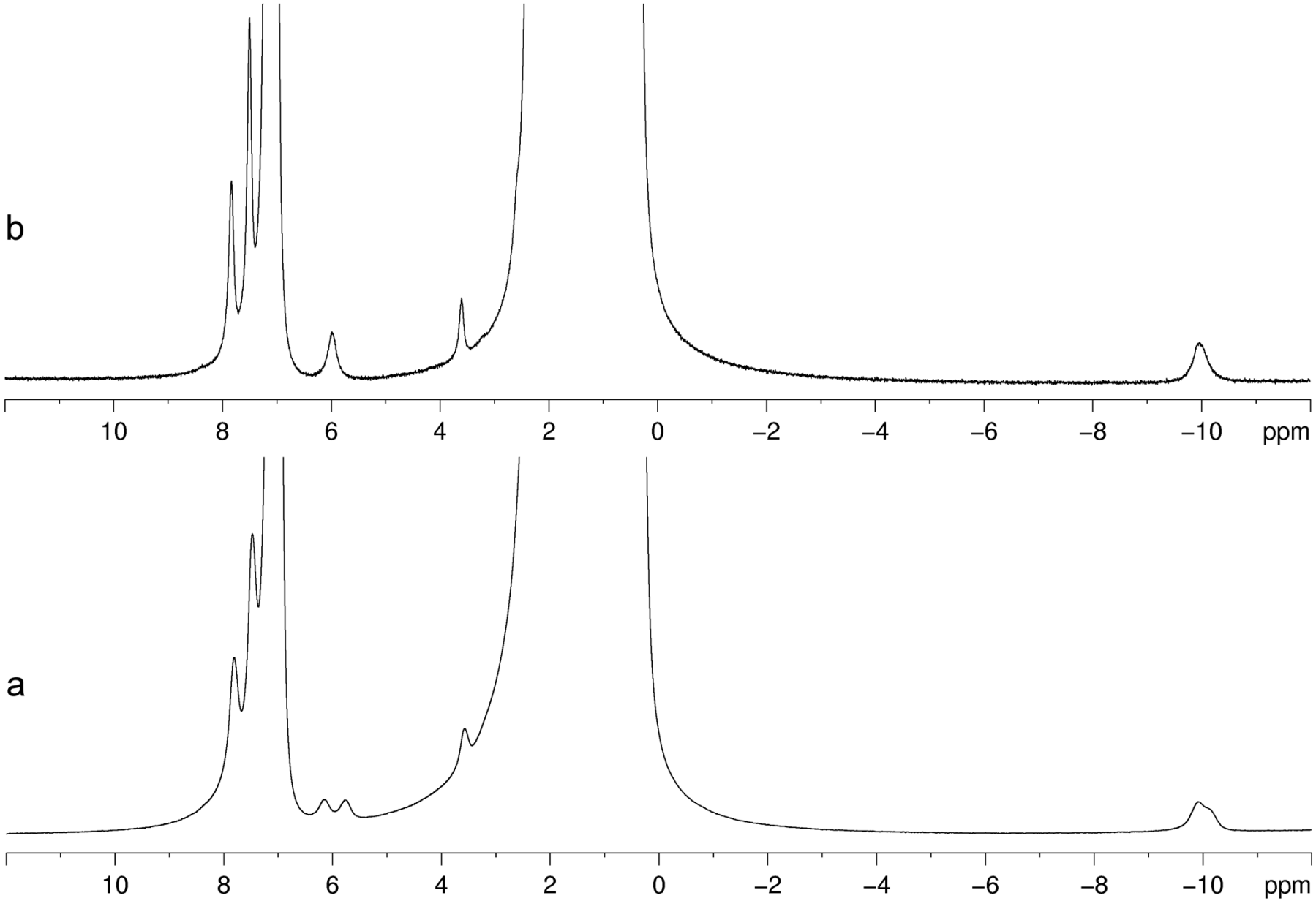

Figure S10. 1D ^{1}H and $^{1}H\{^{31}P\}$ NMR spectra of **2** in toluene-d_8 at T = 193 K.

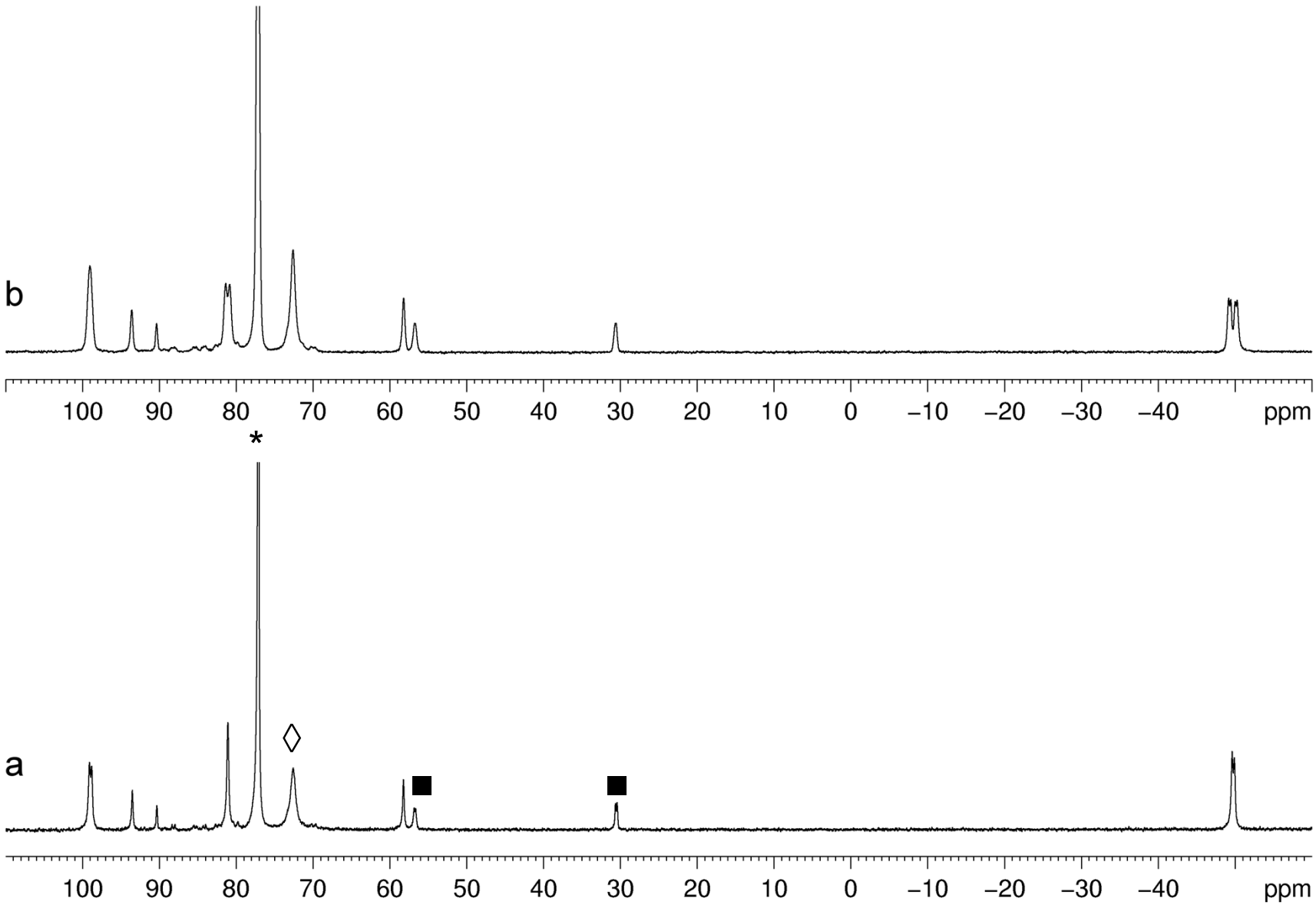

Figure S11. 1D $^{31}P\{^{1}H\}$ and ^{31}P NMR spectra of **2** in toluene-d_8 at T = 193 K (* - $[Ni(dtbpe)(CH_3)_2]$, ◊ - $[\{Ni(dtbpe)\}_2(\mu\text{-}\eta^2\text{:}\eta^2\text{-}C_6D_5CD_3)]$, ■ - $tBu_2P(O)CH_2CH_2PtBu_2$).

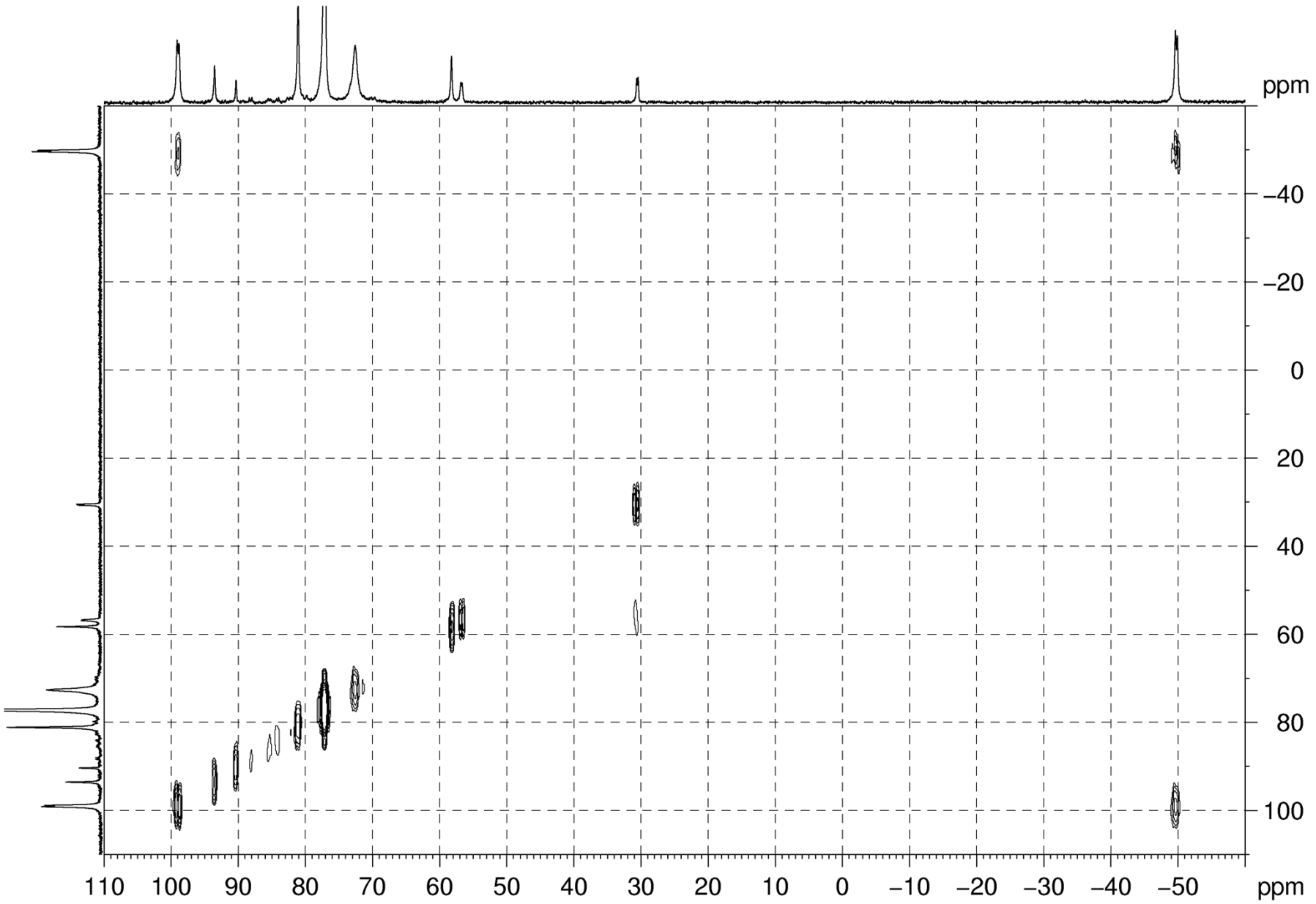

Figure S12. 2D ^{31}P-^{31}P COSY NMR spectra of **2** in toluene-d_8 at T = 193 K.

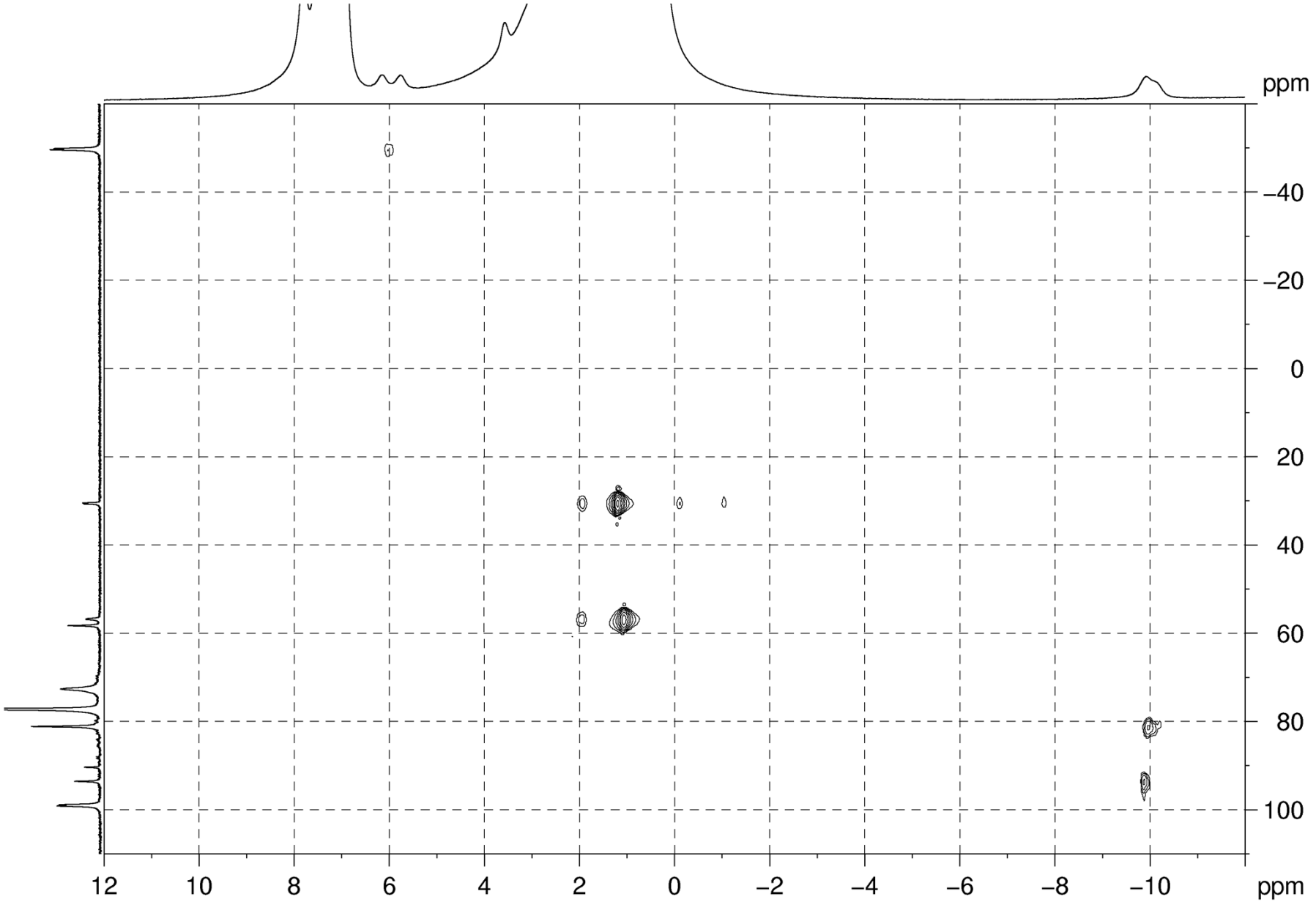

Figure S13. 2D ^{1}H-^{31}P HSQC NMR spectra of **2** in toluene-d_8 at T = 193 K.

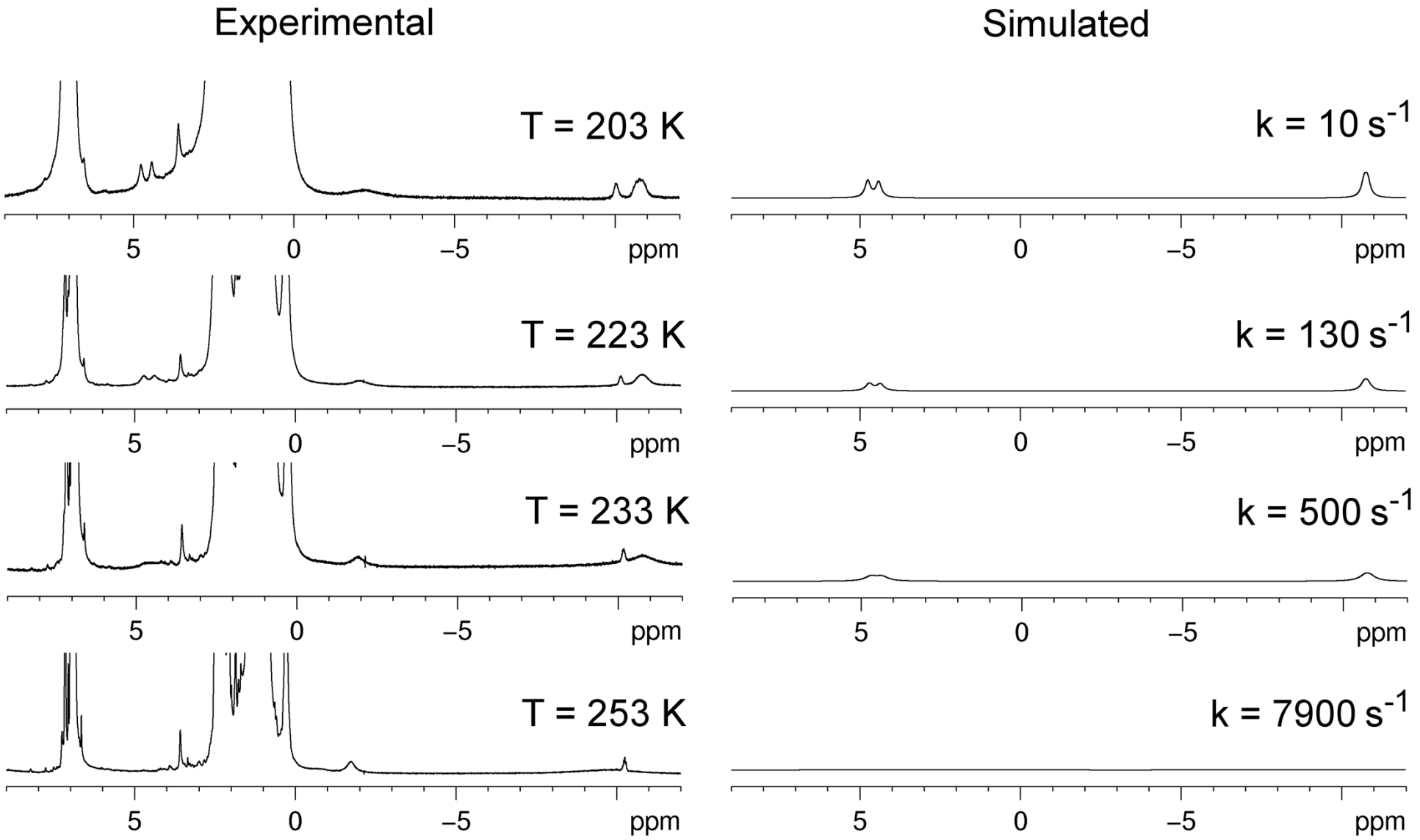

Figure S14. 1D ^{1}H NMR spectra of **1** in toluene-d_8 at different temperatures with corresponding simulated spectra.

Calculations

The quantum chemical calculations were performed using Gaussian 03. Full geometry optimizations have been carried using different approaches: within the framework of DFT functional B3LYP and PBE1PBE employing various basis sets (6-31G(d), 6-31+G(d), 6-31G(d,p), 6-311G(d), 6-311G(2d,p)), and using B3LYP functional employing an ECP basis such as SDD (Stuttgart/Dresden ECP)[1] and LANL2DZ[2] (Los Alamos National Laboratory 2 double zeta) for metals, while using 6-31G(d) and 6-31+G(d) basis sets for all other non-metal atoms. The synchronous transit-guided quasi-newton method was used to locate transition states.[3]

[1] Dolg, M.; Wedig, U.; Stoll, H.; Preuss, H. *J. Chem. Phys.* **1987**, *86*, 866.

[2] Wadt, W. R.; Hay, P. J. *J. Chem. Phys.* **1985**, *82*, 284.

[3] Peng, C.; Ayala, P. Y.; Schlegel, H. B.; Frisch, M. J. *J. Comput. Chem.* **1996**, ***17***, 49.

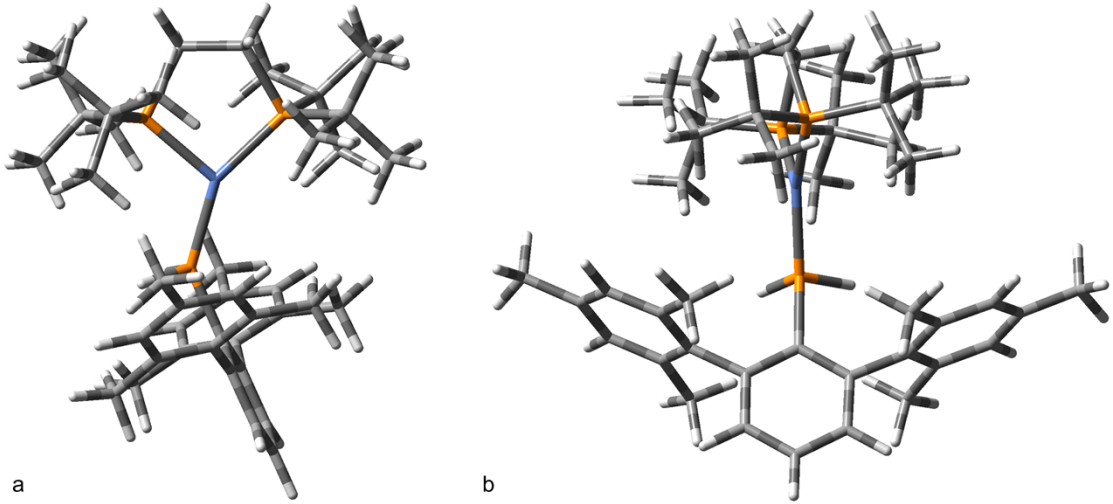

Figure S15. Front view (a) and side view (b) of optimized structure of Ni-PH_2 tautomer of **1** at the B3LYP/6-31+G(d) level of theory (*E* = -4173.1882121 Hartree).

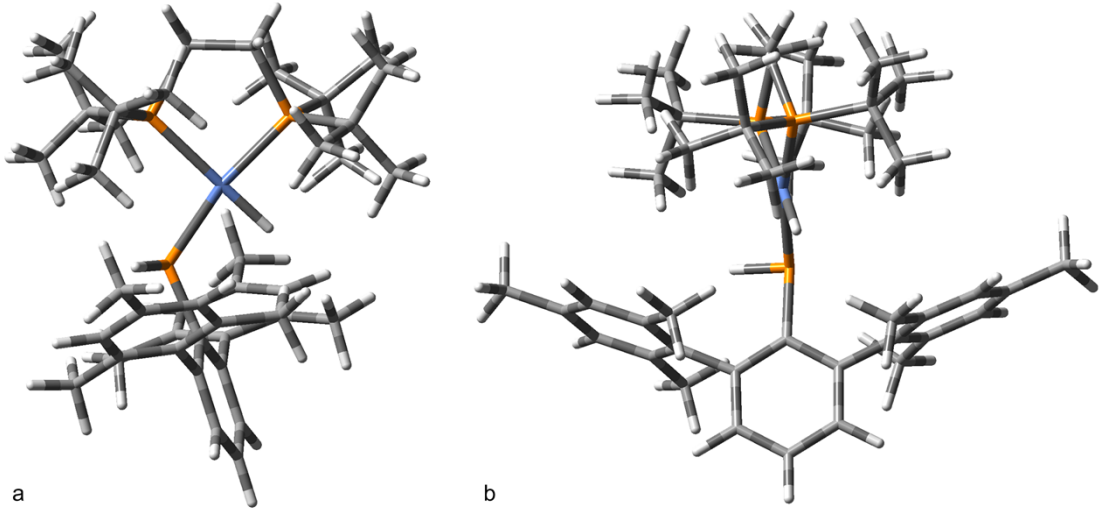

Figure S16. Front view (a) and side view (b) of optimized structure of NiH-PH tautomer of **1** at the B3LYP/6-31+G(d) level of theory (*E* = -4173.1919345 Hartree).

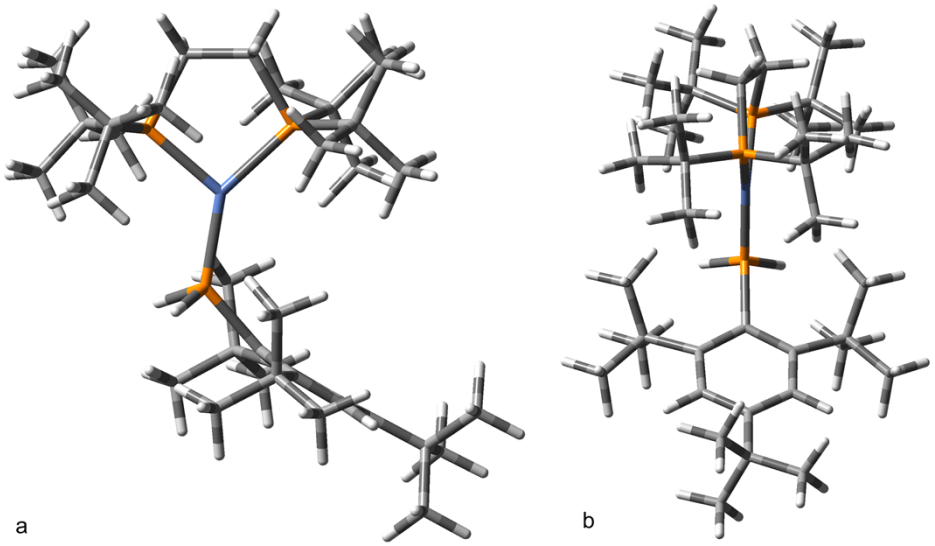

Figure S17. Front view (a) and side view (b) of optimized structure of Ni-PH_2 tautomer of **2** at the B3LYP/6-31+G(d) level of theory (*E* = -3946.9024563 Hartree).

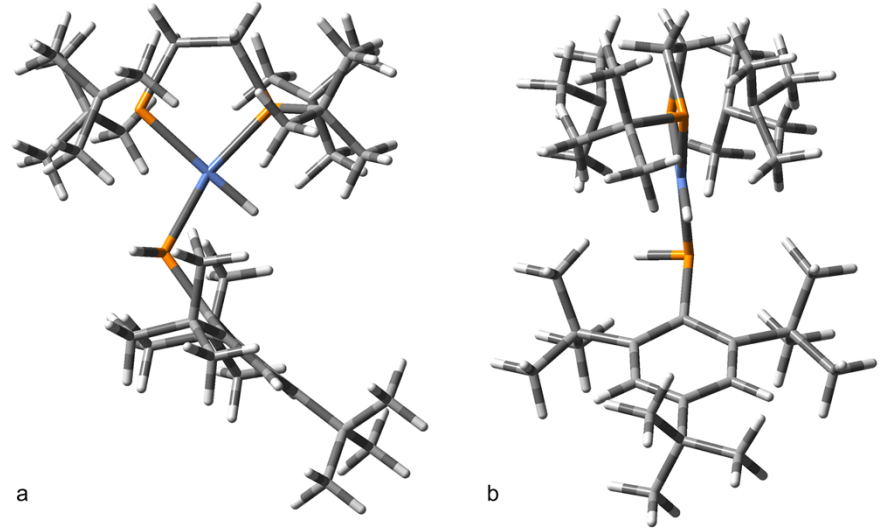

Figure S18. Front view (a) and side view (b) of optimized structure of NiH-PH tautomer of **2** at the B3LYP/6-31+G(d) level of theory (*E* = -3946.9048148 Hartree).

Table S1. Main and transition state energies for compounds [NiH{P(Dmp)(H)}(dtbpe)] (Dmp = 2,6-dimesitylphenyl, **1**), [NiH{P(Mes*)(H)}(dtbpe)] (Mes* = 2,4,6-tri-tert-butyl phenyl, **2**) and [NiH{P(Mes)(H)}(dtbpe)] (Mes = 2,4,6-methyl phenyl).

	Combination	NiH_2-P		NiH-PH		TS_1[a] H-migration		PH_2		TS_2 Rotation barier		TS_3 "Flip-flop" barrier	
		Hartree	kcal/mol	Hartree	kcal/mol	Hartree	kcal/mol	Hartree	kcal/mol	Hartree	kcal/mol	Hartree	kcal/mol
[NiH{P(Dmp)(H)}(dtbpe)] (**1**)													
1	PBE1PBE/6-31G(d)	>-4170.3459629	>39.2	-4170.4085368	0	-4170.3846750	15.0	-4170.3954951	8.2	-4170.3854733	6.2		
2	PBE1PBE/6-31G(d,p)			-4170.3828902	0	-4170.3585851	15.2	-4170.3679799	9.4				
3	PBE1PBE/6-31+G(d)			-4170.4938533	0	-4170.4766052	10.8	-4170.4875865	3.9	-4170.4753778	7.7		
4	B3LYP/6-31G(d)	>-4173.0284390	>41.9	-4173.0953067	0	-4173.0721300	14.5	-4173.0832673	7.6	-4173.0742830	5.6	-4173.06257466	20.5
5	B3LYP/6-31+G(d)	>-4173.1210400	>44.5	-4173.1919345	0	-4173.1765625	9.6	-4173.1882121	2.3	-4173.1776187	9.0	-4173.16864425	14.6
6	B3LYP/6-31G(d)+6d			-4173.0953069	0			-4173.0832672	7.6				
7	B3LYP/6-31G(d,p)			-4173.1937224	0			-4173.1796853	8.8				
8	B3LYP/6-311G(2d,p)			-4173.7873924	0			-4173.7817267	3.6				
9	B3LYP/DZ(d)[b]	>-2834.1744213	>50.7	-2834.2545102	0.5	-2834.2429984	7.7	-2834.2553385	0	-2834.2482120	5.0		
10	B3LYP/combined[c]			-2833.2070726	0			-2833.1923233	9.3				
11	B3LYP/SDD(d)[d]	>-2835.8349620	>44.7	-2835.9062678	0			-2835.9005576	3.6				
12	B3LYP/SDD(d)+[e]	>-2835.8765979	>44.6	-2835.9476990	0			-2835.9419584	3.6				
13	RB3LYP/PCM[f]			-4173.1035020	0	-4173.0765820	16.9	-4173.0876921	9.9				
[NiH{P(Mes*)(H)}(dtbpe)] (**2**)													
14	B3LYP/6-31G(d)	>-3946.7492113	>41.6	-3946.8155146	0	-3946.7974182	11.3	-3946.8052424	6.4	-3946.7884514	11.6	-3946.7858199	18.6
15	B3LYP/6-31G(d,p)	>-3946.8567029	>39.2	-3946.9192866	0			-3946.9069625	7.7				
16	B3LYP/6-31+G(d)	>-3946.8370228	>42.5	-3946.9048148	0	-3946.8926752	7.6	-3946.9024563	1.5	-3946.8923021	7.8	-3946.8833212	13.5
17	B3LYP/6-311G(d)	>-3947.1861240	>46.0	-3947.3152936	0			-3947.3091648	3.8				
18	B3LYP/6-311+G(d)			-3947.3513115	0			-3947.3488307	1.6				
19	B3LYP/DZ(d)[b]	>-2607.9011776	>47.5	-2607.9745691	1.5			-2607.9769293	0				
20	B3LYP/SDD(d)[d]	>-2609.5595332	>41.8	-2609.6261988	0			-2609.6221920	2.5				
21	B3LYP/SDD(d)+[e]	>-2609.5933793	>41.8	-2609.6600318	0			-2609.6563628	2.3				
[NiH{P(Mes)(H)}(dtbpe)]													
22	B3LYP/6-31G(d)			-3593.0432537	0	-3593.0245941	11.7	-3593.0328553	6.5			-3593.0003460	26.9
23	B3LYP/6-31+G(d)			-3593.1248731	0	-3593.1130154	7.4	-3593.1237468	0.7	-3593.1217732	1.9	-3593.0938284	19.5

[a] Transition state for proton migration from Ni to P; [b] B3LYP/{Ni(Lanl2dz); P,C,H(6-31G(d))}; [c] B3LYP/{Ni(valence), P,C,H(6-31G(d))}, Ni (core) - Lanl2dz; [d] B3LYP/{Ni(SDD); P,C,H(6-31G(d))}; [f] B3LYP/{Ni(SDD); P,C,H(6-31+G(d))}; [f] RB3LYP/6-31G(d) with framework of PCM (solvent CHCl3).

Table S2. Influence of metal type on conformational preference of MH-PH ↔ M-PH_2 equilibrium.

Isomer	M = Ni				M = Pd		M = Pt	
	B3LYP/6-31+G(d)		B3LYP/SDD(d)+[a]		B3LYP/SDD(d)+[a]		B3LYP/SDD(d)+[a]	
	E, Hartree	*E*, kcal/mol	*E*, Hartree	*E*, kcal/mol	*E*, Hartree	*E*, kcal/mol	*E*, Hartree	*E*, kcal/mol
[MH{P(Dmp)(H)}(dtbpe)] (**1**)								
NiH-PH	-4173.1921865	0	-2835.9476990	0	-2792.9491987	2.3	-2784.4407311	0
Ni-PH_2	-4173.1882121	2.5	-2835.9419584	3.6	-2792.9528399	0	-2784.4221589	11.6
NiH_2-P	>-4173.1210400	>44.7	>-2835.876598	>44.6	>-2792.8593808	>58.6	>-2784.3679832	>45.6
[MH{P(Mes*)(H)}(dtbpe)] (**2**)								
NiH-PH	-3946.9048148	0	-2609.6600318	0	-2566.6612778	3.3	-2558.1531614	0
Ni-PH_2	-3946.9024563	1.5	-2609.6563628	2.3	-2566.6664813	0	-2558.1365443	10.4
NiH_2-P	>-3946.8370228	>42.5	>-2609.5933793	>41.8	>-2566.5795060	>54.5	>-2558.0863933	>41.9
[MH{P(Mes)(H)}(dtbpe)]								
NiH-PH	-3593.1248731	0	-2255.8804842	0	-2212.8809845	3.8	-2204.3731214	0
Ni-PH_2	-3593.1237468	0.7	-2255.8779560	1.6	-2212.8869649	0	-2204.3575824	9.7

[a] B3LYP/{M(SDD); P,C,H(6-31+G(d))}.

Table S3. Energies of main isomers of [MH{P(Mes*)(Me)}(dtbpe)].

Oxidation state	Isomer	Ni[a]		Ni SDD[b]		Pd SDD[b]		Pt SDD[b]	
		E, Hartree	*E*, kcal/mol	*E*, Hartree	*E*, kcal/mol	*E*, Hartree	*E*, kcal/mol	*E*, Hartree	*E*, kcal/mol
0	M{P(H)(Me)(Mes*)}	-3986.21421058	0	-2648.9679251	0	-2605.9776553	0	-2597.4482157	2.0
0	M{P(Me)(H)(Mes*)}	-3986.2134187	0.5	-2648.9671791	0.5	-2605.9772768	0.2	-2597.4480209	2.2
II	MH{P(Me)(Mes*)}	-3986.2048634	5.9	-2648.9599736	5.0	-2605.9598942	11.1	-2597.4512438	0.1
II	MMe{P(H)(Mes*)}	-3986.1991946	9.4	-2648.9554802	7.8	-2605.9615648	10.1	-2597.4514685	0

[a] B3LYP/6-31+G(d); [b] B3LYP/{M(SDD); P,C,H(6-31+G(d))}.

Table S4. Isomers of [PtH{P(Mes)(Mes)}(dppe)] with corresponding energies[a].

Structure		*E*, Hartree	*E*, kcal/mol
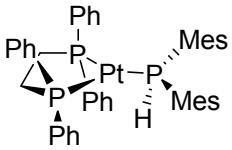	[Pt](PHMesMes)	-2848.59310765	2.3
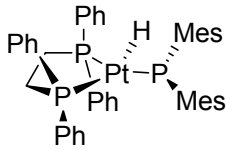	[Pt](H)(PMesMes)	-2848.5943166	1.5
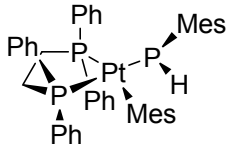	[Pt](Mes)(PHMes)	-2848.59671762	0
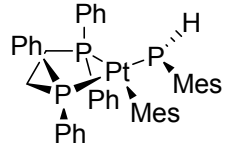	[Pt](Mes)(PMesH)	-2848.59608597	0.4

[a] B3LYP/{Pt(SDD); P,C,H(6-31+G(d))}.